LETTER

doi:10.1038/nature10077

Hf–W–Th evidence for rapid growth of Mars and its status as a planetary embryo

N. Dauphas[1] & A. Pourmand[1,2]

Terrestrial planets are thought to have formed through collisions between large planetary embryos[1] of diameter ~1,000–5,000 km. For Earth, the last of these collisions involved an impact by a Mars-size embryo that formed the Moon 50–150 million years (Myr) after the birth of the Solar System[2,3]. Although model simulations of the growth of terrestrial planets can reproduce the mass and dynamical parameters of the Earth and Venus, they fall short of explaining the small size of Mars[4,5]. One possibility is that Mars was a planetary embryo that escaped collision and merging with other embryos[1]. To assess this idea, it is crucial to know Mars' accretion timescale[6], which can be investigated using the ^{182}Hf–^{182}W decay system in shergottite-nakhlite-chassignite meteorites[6–10]. Nevertheless, this timescale remains poorly constrained owing to a large uncertainty associated with the Hf/W ratio of the Martian mantle[6] and as a result, contradicting timescales have been reported that range between 0 and 15 Myr (refs 6–10). Here we show that Mars accreted very rapidly and reached about half of its present size in only $1.8^{+0.9}_{-1.0}$ Myr or less, which is consistent with a stranded planetary embryo origin. We have found a well-defined correlation between the Th/Hf and ^{176}Hf/^{177}Hf ratios in chondrites that reflects remobilization of Lu and Th during parent-body processes. Using this relationship, we estimate the Hf/W ratio in Mars' mantle to be 3.51 ± 0.45. This value is much more precise than previous estimates, which ranged between 2.6 and 5.0 (ref. 6), and lifts the large uncertainty that plagued previous estimates of the age of Mars. Our results also demonstrate that Mars grew before dissipation of the nebular gas when ~100-km planetesimals, such as the parent bodies of chondrites, were still being formed. Mars' accretion occurred early enough to allow establishment of a magma ocean powered by decay of ^{26}Al.

The age of core formation on Mars can be estimated by measuring the excess abundance of ^{182}W, which is produced from decay of ^{182}Hf, relative to other non-radiogenic isotopes of W in the Martian mantle. Measurements of shergottite–nakhlite–chassignite (SNC) meteorites give a value of $\varepsilon^{182}W_{\text{Mars mantle}} \approx +0.4$ or possibly higher (here ε^{182}W is the deviation in 0.01% of the ^{182}W/^{183}W or ^{182}W/^{184}W ratio relative to the terrestrial mantle)[6–10]. In addition to ε^{182}W, the Hf/W ratio of Mars' mantle is also needed to calculate the age of core formation. This ratio, however, cannot be measured directly in SNC meteorites because Hf and W behave differently during mantle melting and crystallization. Instead, the mantle Hf/W ratio can be calculated as $(Hf/W)_{\text{Mars mantle}} = (Th/W)_{\text{Mars mantle}}/(Th/Hf)_{\text{Mars mantle}}$. In most circumstances, Th and W have similar magmatic behaviours[6]. Despite different sources and chemical compositions, the average Th/W ratios of shergottites and nakhlites are identical within uncertainties (that is, 0.68 ± 0.09 versus 0.79 ± 0.32, Supplementary Table 1). This shows that there is no relationship between measured Th/W ratios and the inferred mineralogy of the mantle source region (for example, the presence of clinopyrexene, garnet or ilmenite[11,12]). There is also no relationship between Th/W ratios and geochemical proxies of magmatic fractionation[6]. Therefore, $(Th/W)_{\text{Mars mantle}}$ can be approximated by the average value of SNC meteorites, $(Th/W)_{\text{Mars mantle}} = (Th/W)_{\text{SNC}} = 0.752 \pm 0.092$ (Supplementary Table 1). As refractory lithophile elements, Th and Hf are expected to be in chondritic proportions (CHUR, chondritic uniform reservoir) in the Martian mantle, hence, $(Th/Hf)_{\text{Mars mantle}} = (Th/Hf)_{\text{CHUR}}$. It follows that:

$$(Hf/W)_{\text{Mars mantle}} = (Th/W)_{\text{SNC}}/(Th/Hf)_{\text{CHUR}} \quad (1)$$

The main source of uncertainty in the age of Mars is the Th/Hf ratio in chondrites that varies by a factor of >3 (ref. 6, this study). In order to address this problem, we have measured elemental concentrations (U, Th, Lu and Hf) and isotopic compositions (^{176}Hf/^{177}Hf) of 44 chondrites, mainly falls, covering all major chondrite groups (Table 1). The elemental concentrations were measured by isotope dilution; the methodology is described in Methods Summary. The meteorites define a clear correlation in Th/Hf versus ^{176}Hf/^{177}Hf space (Fig. 1). The ^{176}Hf/^{177}Hf ratio is another proxy for Lu/Hf ratio, as ^{176}Lu decays to ^{176}Hf with a half-life of 36.8 Gyr (refs 13, 14). The variations in Hf isotopic composition of ordinary chondrites have been interpreted to reflect redistribution of Lu during parent-body metamorphism[14]. Lu, U and Th are concentrated in trace carrier phases like phosphates (chlorapatite and merrillite) for ordinary as well as carbonaceous chondrites, and sulphides (oldhamite) for enstatite chondrites (refs 15, 16 and references therein). Variations in the abundance of these trace phases at the bulk sample scale due to parent-body redistribution during metamorphism (that is, a nugget effect; Fig. 1b) is the most likely cause for the observed correlation in Fig. 1a. The chondritic ^{176}Hf/^{177}Hf isotopic ratio (~0.282785) is well known from measurement of chondrites of low metamorphic grade[14]. We can therefore use this ratio and the correlation presented in Fig. 1a to calculate $(Th/Hf)_{\text{Mars mantle}} = (Th/Hf)_{\text{CHUR}} = 0.2144 \pm 0.0075$. This translates to a precise estimate of 3.51 ± 0.45 for the Hf/W ratio of the Martian mantle (equation (1)).

If Mars was a stranded embryo formed by accretion of planetesimals during runaway and oligarchic growth (see below), its mass at any given time can be parameterized as[17,18]

$$M_{\text{Mars}}(t)/M_{\text{Mars}} = \tanh^3(t/\tau) \quad (2)$$

where t is counted from the formation of the Solar System (that is, the condensation of calcium-aluminium-rich inclusions, CAIs, in meteorites), and τ is the accretion timescale. At $t = \tau$, the embryo reached $\tanh^3(1) = 44\%$ of its present size. On Earth, the extent to which 1,000–5,000-km planetary embryos striking the surface equilibrated with the mantle of the protoplanet is uncertain. Modelling and geochemical considerations, however, suggest that incomplete equilibration on Earth affected Hf–W chronology[19,20]. If Mars were an embryo, its accretion would have proceeded by collisions with 10–100-km planetesimals that were much smaller than the target embryo. In addition, Mars would have formed early enough to develop a magma ocean from the heat released by ^{26}Al decay (<2.5 Myr after

[1]Origins Laboratory, Department of the Geophysical Sciences and Enrico Fermi Institute, The University of Chicago, 5734 South Ellis Avenue, Chicago, Illinois 60637, USA. [2]Rosenstiel School of Marine & Atmospheric Science, Division of Marine Geology and Geophysics, University of Miami, 4600 Rickenbacker Causeway, Miami, Florida 33149, USA.

Table 1 | U–Th–Lu–Hf systematics of chondrites

Meteorite name	Meteorite group	Fall	Source	Collection ID	U ($ng\,g^{-1}$)	Th ($ng\,g^{-1}$)	Hf ($ng\,g^{-1}$)	Lu ($ng\,g^{-1}$)	$^{176}Hf/^{177}Hf$ (JMC-normalized)	Lu/Hf atomic ratio	Th/Hf atomic ratio	Th/U atomic ratio	Lu/Th atomic ratio
Ivuna	CI1	Yes	USNM	6630	8.29	31.85	116.22	27.99	0.282826	0.2457	0.2108	3.94	1.166
Mighei	CM2	Yes	FM	1456	10.64	37.69	139.05	33.01	0.282795	0.2421	0.2085	3.63	1.161
Kainsaz	CO3.2	Yes	FM	2755	13.73	48.00	186.17	43.75	0.282817	0.2397	0.1983	3.59	1.209
Lancé	CO3.5	Yes	FM	1351	16.18	47.27	177.31	41.46	0.282762	0.2385	0.2051	3.00	1.163
Allende	CV3	Yes	USNM	3529	15.34	58.19	192.17	46.02	0.282835	0.2443	0.2329	3.89	1.049
Allende	CV3	Yes	USNM	3529	16.00	58.04	192.16	45.92	0.282795	0.2438	0.2323	3.72	1.049
Allende	CV3	Yes	USNM	3529	15.71	58.90	189.49	45.24	0.282839	0.2436	0.2391	3.85	1.019
Allende	CV3	Yes	USNM	3529	15.38	59.75	205.55	48.54	0.282814	0.2409	0.2236	3.98	1.077
Allende*	CV3	Yes	USNM	3529	15.58	59.80	192.93	46.03	0.282824	0.2434	0.2384	3.94	1.021
Allende*	CV3	Yes	USNM	3529	15.23	58.37	192.70	46.43	0.282795	0.2458	0.2330	3.93	1.055
Allende*	CV3	Yes	USNM	3529	15.57	57.42	192.20	46.12	0.282801	0.2448	0.2298	3.78	1.065
Grosnaja	CV3	Yes	FM	1732	23.61	61.50	161.60	39.07	0.282811	0.2466	0.2927	2.67	0.843
Vigarano	CV3	Yes	FM	782	14.66	53.49	207.07	49.15	0.282789	0.2421	0.1987	3.74	1.219
Sahara 97072	EH3	No	Private collection	NA	8.92	28.40	111.02	25.27	0.282748	0.2322	0.1968	3.27	1.180
Qingzhen	EH3	Yes	R.N. Clayton	NA	7.61	25.84	107.09	24.50	0.282704	0.2334	0.1856	3.48	1.257
Indarch	EH4	Yes	FM	3466	9.44	27.37	104.49	23.45	0.282685	0.2290	0.2015	2.97	1.136
Adhi Kot	EH4	Yes	AMNH	3993	7.86	26.76	73.31	23.92	0.284055	0.3329	0.2808	3.49	1.186
St. Mark's	EH5	Yes	USNM	3027	8.39	27.60	87.68	23.18	0.283143	0.2697	0.2421	3.38	1.114
Saint-Sauveur	EH5	Yes	MNHN	1456	7.62	24.40	76.07	20.31	0.283250	0.2724	0.2468	3.29	1.104
Daniel's Kuil	EL6	Yes	FM	1500	8.14	29.34	138.16	29.26	0.282528	0.2161	0.1633	3.70	1.323
Yilmia	EL6	No	FM	2740	5.53	23.05	117.58	23.41	0.282331	0.2031	0.1508	4.28	1.347
Blithfield	EL6	No	FM	1646	18.75	48.31	103.66	34.24	0.284231	0.3369	0.3585	2.64	0.940
Hvittis	EL6	Yes	FM	578	6.82	31.89	134.41	30.38	0.282651	0.2306	0.1825	4.80	1.263
Eagle	EL6	Yes	FM	3149	7.56	31.05	176.23	31.20	0.281972	0.1806	0.1356	4.22	1.332
Khairpur	EL6	Yes	FM	1538	6.84	25.77	137.20	24.05	0.282061	0.1788	0.1445	3.86	1.237
Pillistfer	EL6	Yes	FM	1647	5.82	25.16	112.72	24.97	0.282648	0.2260	0.1717	4.43	1.316
Jajh Deh Kot Lalu	EL6	Yes	USNM	1260	4.90	24.27	158.95	22.88	0.281675	0.1468	0.1175	5.08	1.250
Happy Canyon	EL6/7	No	FM	2760	189.63	30.47	141.55	23.12	0.281758	0.1666	0.1656	0.16	1.006
Ilafegh 009	EL7	No	AMNH	4757	5.48	26.19	100.26	24.04	0.282726	0.2446	0.2009	4.90	1.218
Bielokrynitschie	H4	Yes	FM	1394	12.17	40.79	144.31	31.37	0.282581	0.2218	0.2174	3.44	1.020
Ochansk	H4	Yes	FM	1443	11.63	39.46	151.14	33.96	0.282699	0.2292	0.2008	3.48	1.141
Kesen	H4	Yes	FM	1822	12.71	38.79	132.67	32.36	0.282849	0.2489	0.2249	3.13	1.106
Kernouve	H6	Yes	MNHN	602	12.03	35.68	128.88	29.30	0.282695	0.2319	0.2130	3.04	1.089
Dalgety Downs	L4	No	FM	2613	21.87	49.11	144.68	31.79	0.282371	0.2242	0.2611	2.30	0.859
Bald Mountain	L4	Yes	FM	2392	10.45	38.36	147.24	37.14	0.283005	0.2573	0.2004	3.77	1.284
Barratta	L4	No	FM	1463	13.50	38.71	148.75	34.66	0.282760	0.2377	0.2002	2.94	1.187
Farmington	L5	Yes	FM	347	20.73	53.82	148.21	44.17	0.283741	0.3040	0.2793	2.66	1.088
Harleton	L6	Yes	FM	2686	8.83	34.56	150.25	31.96	0.282421	0.2170	0.1769	4.01	1.226
Hamlet	LL4	Yes	FM	3296	12.98	47.57	177.02	39.01	0.282619	0.2248	0.2067	3.76	1.087
Kelly	LL4	No	FM	2235	15.07	38.50	119.33	32.18	0.283067	0.2751	0.2481	2.62	1.109
Soko-Banja	LL4	Yes	FM	1374	12.42	39.01	149.07	33.83	0.282722	0.2315	0.2013	3.22	1.150
Tuxtuac	LL5	Yes	FM	2850	18.01	50.03	168.49	38.91	0.282619	0.2356	0.2284	2.85	1.032
Paragould	LL5	Yes	FM	2135	21.61	58.41	171.60	45.16	0.283217	0.2684	0.2618	2.77	1.025
Saint-Séverin	LL6	Yes	MNHN	2397	11.16	47.64	184.68	42.70	0.282735	0.2358	0.1984	4.38	1.189

Concentration measurements were carried out by isotope dilution mass spectrometry. The absolute uncertainties (2σ, 95% confidence intervals calculated from replicate analyses of Allende) are ±0.52 (U), ±1.78 (Th), ±10.54 (Hf), ±2.08 (Lu), ±0.000036 ($^{176}Hf/^{177}Hf$), ±0.0030 (Lu/Hf), ±0.0105 (Th/Hf), ±0.19 (Th/U) and ±0.043 (Lu/Th). 'JMC-normalized' refers to JMC-475 (see Methods for details). Happy Canyon has a high U/Th ratio, reflecting terrestrial contamination, and was not used in calculation of the Th/Hf ratio of CHUR. NA, not available.
* Samples were digested by high-pressure HF bomb. All other samples were digested by flux fusion.

CAIs, ref. 21), and the planetesimals striking its surface would have also been molten. The fact that the impactors were molten and that they were much smaller than the target embryo would have led to vaporization of the planetesimals upon impact and equilibration with the mantle of proto-Mars. Under this reasonable assumption, we can predict the excess in radiogenic ^{182}W of the mantle relative to chondrites for various accretion timescales (values of τ)[9]:

$$\varepsilon^{182}W_{\text{Mars mantle}} - \varepsilon^{182}W_{\text{CHUR}} = q_W \left(\frac{^{182}Hf}{^{180}Hf}\right)_0 f^{Hf/W}_{\text{Mars mantle}} \lambda \int_0^{4{,}568\text{Myr}} e^{-\lambda t} \tanh^{3+3f^{Hf/W}_{\text{Mars mantle}}}(t/\tau)\, dt \quad (3)$$

All parameters except $f^{Hf/W}_{\text{Mars mantle}} = (Hf/W)_{\text{Mars mantle}}/(Hf/W)_{\text{CHUR}} - 1 = 3.38 \pm 0.56$ were known before this work; $\varepsilon^{182}W_{\text{CHUR}} = -2.23 \pm 0.11$, $q_W = (^{180}Hf/^{182}W)_{\text{CHUR}} \times 10^4 = 1.07 \times 10^4$, $(^{182}Hf/^{180}Hf)_0 = (9.72 \pm 0.44) \times 10^{-5}$, and λ, the decay constant of ^{182}Hf, is $0.0779 \pm 0.0008\ Myr^{-1}$ (refs 7, 10, 22; see Supplementary Information for details). A mixture of 85% H, 11% CV and 4% CI chondrites is chosen for CHUR, which was previously proposed as a model composition for bulk Mars[23]. These mixing proportions influence the values q_W, $\varepsilon^{182}W_{\text{CHUR}}$ and Hf/W_{CHUR}. The W isotopic composition of the Martian mantle is uncertain because different Martian meteorites show variable $\varepsilon^{182}W$ values (from +0.3 to +3). This reflects fractionation of the Hf/W ratio in the Martian magma ocean while ^{182}Hf was still present[7–10].

We adopt a conservative approach by using the least radiogenic W isotopic compositions (lowest $\varepsilon^{182}W$ value) of $\varepsilon^{182}W_{\text{Mars mantle}} = +0.45 \pm 0.15$ (refs 8, 10) proposed for the bulk Martian mantle. Higher values such as those documented in nakhlites would translate to a shorter accretion time. Therefore, the timescale that we calculate is a robust upper limit. To reproduce $\varepsilon^{182}W_{\text{Mars mantle}} = +0.45 \pm 0.15$, we calculate $\tau = 1.8^{+0.9}_{-1.0}$ Myr (Fig. 2), where the error bar (yellow band) represents the 95% confidence interval and is obtained by propagating the uncertainties on $\varepsilon^{182}W_{\text{Mars mantle}}$, $\varepsilon^{182}W_{\text{CHUR}}$, $(^{182}Hf/^{180}Hf)_0$, $f^{Hf/W}_{\text{Mars mantle}}$ and λ, using a Monte Carlo simulation. Assuming a different composition for CHUR would not change the results significantly (for example, $\tau = 2.0^{+1.0}_{-1.2}$ Myr for 100% CI). Scenarios that invoke late-stage accretion of a large body to explain Mars' hemispheric dichotomy[24] could increase model ages in the case of incomplete W isotope equilibration between the impactor and the Martian mantle.

As seen in Fig. 2, most of the accretion of Mars took place during the first 4 Myr of the formation of the Solar System. The accretion

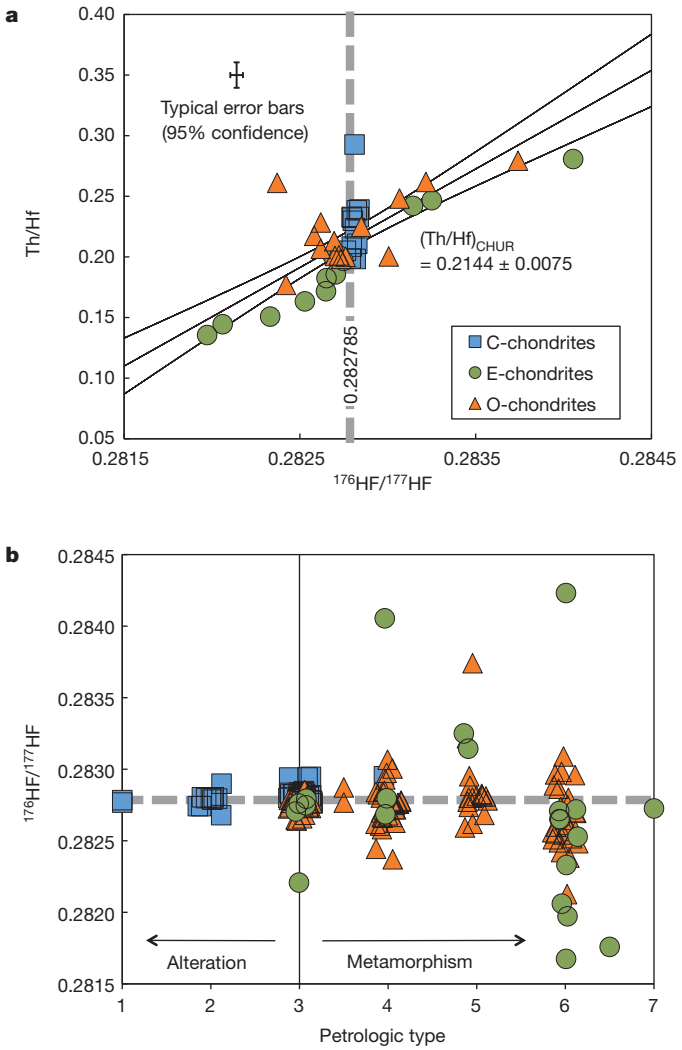

Figure 1 | Determination of the Th/Hf ratio of CHUR. **a**, Correlation between Th/Hf and $^{176}Hf/^{177}Hf$ (a proxy for Lu/Hf) ratios in chondrites (Table 1; C, carbonaceous; E, enstatite; O, ordinary; meteorite Happy Canyon not included). The $^{176}Hf/^{177}Hf$ ratio of CHUR is estimated to be 0.282785 ± 0.000011 (ref. 14), allowing us to estimate $(Th/Hf)_{CHUR} = 0.2144 \pm 0.0075$ (the uncertainty is the 95% confidence interval based on regression of the data). At a Th/Hf ratio of 0, we calculate a $^{176}Hf/^{177}Hf$ ratio of ~0.280, which is close to the Solar System initial ratio of 0.27978 (ref. 14). There is no correlation between the Lu/Th and Lu/Hf ratios (Table 1). These two observations suggest that Th behaves very similarly to Lu but that both elements can be decoupled from Hf in meteorites. If chondrite parent bodies had begun with different Th/Hf ratios (for example, owing to evaporation/condensation processes in the nebula), they would not define a single correlation line. **b**, $^{176}Hf/^{177}Hf$ ratios of chondrites as a function of petrologic types (data from Table 1, refs 12, 13 and references therein). The data points have been moved horizontally by random values to decrease overlap and improve readability. The degree of aqueous alteration increases from type 3 to 1, while the degree of thermal metamorphism increases from type 3 to 7 (that is, the most pristine samples are of type 3). The dispersion in $^{176}Hf/^{177}Hf$ ratios of metamorphosed chondrites (types 4–7) is much larger compared with other samples, indicating that redistribution during parent-body metamorphism is the most likely explanation for the dispersion in Lu/Hf (and Th/Hf) ratios measured in bulk chondrite specimens. The average Th/Hf ratio of unmetamorphosed chondrites (types 1–3) is 0.2217 ± 0.0135, identical within uncertainties with the value derived from the regression in **a**.

timescale of Mars can be compared with those of planetesimals, whose formation history is known from measurement of meteorites. The parent bodies of iron meteorites were formed at the same time or soon after CAIs[10]. Chondrites, which formed >3 Myr after CAIs[25], contain pristine materials such as CAIs and presolar grains that indicate they

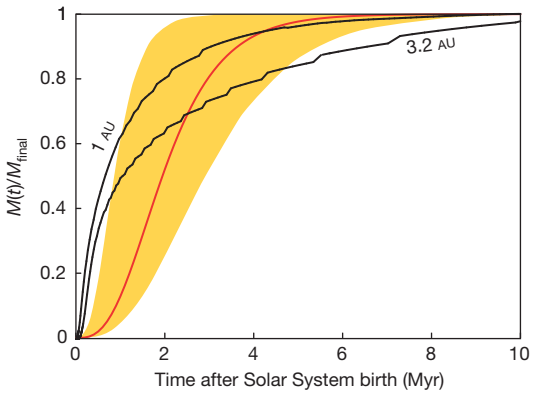

Figure 2 | Accretion timescale of Mars inferred from ^{182}Hf–^{182}W systematics. The red curve is calculated from $M(t)/M_{final} = \tanh^3(t/\tau)$ with $\tau = 1.8^{+0.9}_{-1.0}$ Myr (see text for details). The yellow band corresponds to the 95% confidence interval on the accretion curve of Mars obtained by propagating all uncertainties on model parameters using a Monte Carlo simulation. The two black curves are model simulations of embryo growth at 1 and 3.2 AU (ref. 26) for comparison.

accreted from pristine nebular dust, rather than from collisional debris. Detailed thermochronology also shows that chondrites' parent bodies were probably around 100 km in size[21]. An important finding of this work, therefore, is that large planetesimals (for example, 10–100-km bodies) were still being formed in the protoplanetary disk during Mars' accretion.

The accretion of planetary embryos from planetesimals began with a period of runaway growth, in which large bodies accreted at a much higher rate than smaller ones. When the larger bodies (that is, embryos) became massive enough to dynamically stir the planetesimals around them, their growth was slowed down by reduced gravitational focusing factors, a process known as 'oligarchic growth'. The embryos eventually cleared their orbits of smaller objects, limiting their mass to Moon- to Mars-sized objects. Computer simulations predict that the growth of embryos at 1.5 astronomical units (AU) from the Sun should occur on a maximal timescale of a few million years (note that this timescale is sensitive to the assumed initial surface density)[17,18,26]. The growth of terrestrial planets such as Earth, on the other hand, is thought to have proceeded by collisions between these embryos on an expected timescale of several tens of millions of years, a process known as 'chaotic growth'[1,5]. This timescale on Earth is best constrained by the age of the Moon, which is thought to have formed by a collision that occurred 50–150 Myr after CAIs[3] between a Mars-size planetary embryo and the proto-Earth[2]. It is difficult to reconcile Mars' accretion timescale based on the $\varepsilon^{182}W$ data ($\tau = 1.8^{+0.9}_{-1.0}$ Myr) with an Earth-like mode of accretion. Our findings, however, are entirely consistent with the timescale predicted by models of oligarchic growth (Fig. 2). We therefore conclude that Mars is most likely to be an embryo that escaped collisions and merging with other bodies, thus explaining its small mass compared to Earth and Venus.

Rapid accretion of Mars also has important implications for its magmatic history. The gravitational energy deposited on the growing embryo from planetesimals during oligarchic growth would not have been sufficient to cause large-scale melting[27], except for a mode of runaway core formation triggered by impacts with >3,500-km embryos[28]. In this scheme, the temperature rise would not have been sufficient to induce silicate melting, and molten metal would have segregated through a solid matrix. The Martian mantle (based on the composition of SNC meteorites) contains large ^{182}W and ^{142}Nd isotopic heterogeneities that arise from magmatic fractionation of Hf/W and Sm/Nd while ^{182}Hf and ^{146}Sm (half-life 103 Myr) were still present[7,8,29,30]. The event that caused this chemical fractionation is dated at ~20–60 Myr after CAIs, and may correspond to crystallization of a magma ocean on Mars. A similar age range is obtained from

^{129}I–^{244}Pu–Xe systematics of SNC meteorites, indicating rapid degassing of the Martian mantle[31]. Thermal modelling shows that planetary bodies accreted before ~2.5 Myr would have incorporated enough of the short-lived nuclide ^{26}Al (half-life 0.717 Myr) for radioactive decay (3.16 MeV per decay) to induce silicate melting[21]. Mars would have reached 69±30% of its present size by that time and the heat generated from ^{26}Al decay alone would have been sufficient to establish a magma ocean.

Finally, the idea that Mars was a planetary embryo may also explain the similarities between some characteristics of the terrestrial and Martian atmospheres in spite of marked differences in their sizes and accretion histories. The atmospheres of both planets share what is commonly referred to as the 'missing xenon problem'; on both planets, Xe is isotopically fractionated by 3–4% per AMU relative to the solar value and to that in chondrites, the Xe/Kr ratio is close to the solar value, and Kr is only slightly fractionated[32]. If hydrodynamic escape were responsible for isotopic fractionation of noble gases in the terrestrial planet atmospheres, one would expect more depletion and higher isotopic fractionation in lighter Kr compared with Xe, which is the opposite to what is actually observed. In some models that attempt to explain this problem quantitatively, the similarity between Mars and Earth is taken as a coincidence[32,33]. Alternatively, if Mars was a planetary embryo, as suggested by our findings, Earth may have inherited its missing Xe problem from the atmosphere of a Mars-like planetary embryo, possibly the impactor that also formed the Moon. This idea is consistent with the time when Earth became retentive for Xe, which is estimated to be ~100 Myr after the birth of the Solar System and may correspond to the time of the Moon-forming giant impact[19].

METHODS SUMMARY

About 100 mg of homogenized powder was fused with ultra-pure lithium metaborate (+LiBr) in high-purity graphite crucibles at 1,070 °C for 12 min. The fusion melt was dissolved and spiked with a calibrated ^{236}U–^{229}Th–^{176}Lu–^{180}Hf solution for isotope dilution mass spectrometry (IDMS). After sample–spike equilibration and separation of matrix elements on a 2-ml Eichrom TODGA cartridge, Hf, U and Th were eluted in 3 mol l^{-1} HNO_3 + 0.3 mol l^{-1} HF at 65 °C. Lu was eluted in 0.5 mol l^{-1} HCl and was further purified from heavy rare earth elements, using a 2-ml Eichrom Ln cartridge. The solutions were evaporated and the residues were redissolved in 0.4 mol l^{-1} HNO_3 + 0.04 mol l^{-1} HF for Hf, U and Th, and 0.4 mol l^{-1} HNO_3 for Lu. About 90% of the Hf–U–Th solution was used for concentration and high-precision isotope analysis of Hf, while 10% was analysed for U and Th concentrations by IDMS. All the measurements were done on a Neptune multi-collector inductively coupled plasma mass spectrometer at the University of Chicago. Meteorites and geostandards of known Hf isotopic and U–Th–Lu–Hf elemental compositions were measured to validate the method. Uncertainties (2σ, 95% confidence intervals) were calculated on the basis of replicate analyses of the Allende CV3 chondrite.

Full Methods and any associated references are available in the online version of the paper at www.nature.com/nature.

Received 20 October 2010; accepted 22 March 2011.

1. Chambers, J. E. & Wetherill, G. W. Making the terrestrial planets: *N*-body integrations of planetary embryos in three dimensions. *Icarus* **136,** 304–327 (1998).
2. Canup, R. M. & Asphaug, E. Origin of the Moon in a giant impact near the end of the Earth's formation. *Nature* **412,** 708–712 (2001).
3. Touboul, M., Kleine, T., Bourdon, B., Palme, H. & Wieler, R. Late formation and prolonged differentiation of the Moon inferred from W isotopes in lunar metals. *Nature* **450,** 1206–1209 (2007).
4. Wetherill, G. W. Why isn't Mars as big as Earth? *Lunar Planet. Sci.* **XXII,** 1495–1496 (1991).
5. Raymond, S. N., O'Brien, D. P., Morbidelli, A. & Kaib, A. Building the terrestrial planets: constrained accretion in the inner solar system. *Icarus* **203,** 644–662 (2009).
6. Nimmo, F. & Kleine, T. How rapidly did Mars accrete? Uncertainties in the Hf-W timing of core formation. *Icarus* **191,** 497–504 (2007).
7. Kleine, T., Mezger, K., Münker, C., Palme, H. & Bischoff, A. ^{182}Hf-^{182}W isotope systematics of chondrites, eucrites, and martian meteorites: chronology of core formation and early mantle differentiation in Vesta and Mars. *Geochim. Cosmochim. Acta* **68,** 2935–2946 (2004).
8. Foley, C. N. *et al.* The early differentiation history of Mars from ^{182}W-^{142}Nd isotope systematics in the SNC meteorites. *Geochim. Cosmochim. Acta* **69,** 4557–4571 (2005).
9. Jacobsen, S. B. The Hf-W isotopic system and the origin of the Earth and Moon. *Annu. Rev. Earth Planet. Sci.* **33,** 531–570 (2005).
10. Kleine, T. *et al.* Hf-W chronology of the accretion and early evolution of asteroids and terrestrial planets. *Geochim. Cosmochim. Acta* **73,** 5150–5188 (2009).
11. Righter, K. & Shearer, C. K. Magmatic fractionation of Hf and W: constraints on the timing of core formation and differentiation in the Moon and Mars. *Geochim. Cosmochim. Acta* **67,** 2497–2507 (2003).
12. Bouvier, A., Blichert-Toft, J. & Albarède, F. Martian meteorite chronology and evolution of the interior of Mars. *Earth Planet. Sci. Lett.* **280,** 285–295 (2009).
13. Blichert-Toft, J. & Albarède, F. The Lu-Hf isotope geochemistry of chondrites and the evolution of the mantle-crust system. *Earth Planet. Sci. Lett.* **148,** 243–258 (1997).
14. Bouvier, A., Vervoort, J. D. & Patchett, P. J. The Lu-Hf and Sm-Nd isotopic composition of CHUR: constraints from unequilibrated chondrites and implications for the bulk composition of terrestrial planets. *Earth Planet. Sci. Lett.* **273,** 48–57 (2008).
15. Goreva, J. S. & Burnett, D. S. Phosphate control on the thorium/uranium variations in ordinary chondrites: improving solar system abundances. *Meteorit. Planet. Sci.* **36,** 63–74 (2001).
16. Murrell, M. T. & Burnett, D. S. Actinide microdistributions in the enstatite meteorites. *Geochim. Cosmochim. Acta* **46,** 2453–2460 (1982).
17. Thommes, E. W., Duncan, M. J. & Levison, H. F. in *Astrophysical Ages and Time Scales* (eds von Hippel, T., Simpson, C. & Manset, N.) 91–100 (ASP Conference Series Vol. 245, Astronomical Society of the Pacific, 2001).
18. Chambers, J. A semi-analytic model for oligarchic growth. *Icarus* **180,** 496–513 (2006).
19. Halliday, A. N. Mixing, volatile loss and compositional change during impact-driven accretion of the Earth. *Nature* **427,** 505–509 (2004).
20. Dahl, T. W. & Stevenson, D. J. Turbulent mixing of metal and silicate during planetary accretion — an interpretation of the Hf-W chronometer. *Earth Planet. Sci. Lett.* **295,** 177–186 (2010).
21. Grimm, R. E. & McSween, H. Y. Jr. Heliocentric zoning of the asteroid belt by aluminum-26 heating. *Science* **259,** 653–655 (1993).
22. Yin, Q. *et al.* A short timescale for terrestrial planet formation from Hf-W chronometry of meteorites. *Nature* **418,** 949–952 (2002).
23. Lodders, K. & Fegley, B. Jr. An oxygen isotope model for the composition of Mars. *Icarus* **126,** 373–394 (1997).
24. Wilhelms, D. E. & Squyres, S. W. The martian hemispheric dichotomy may be due to a giant impact. *Nature* **309,** 138–140 (1984).
25. Kita, N. T. *et al.* in *Chondrites and the Protoplanetary Disk* (eds Krot, A. N., Scott, E. R. D. & Reipurth, B.) 558–587 (ASP Conference Series Vol. 341, Astronomical Society of the Pacific, 2005).
26. Kobayashi, H., Tanaka, H., Krivov, A. V. & Inaba, S. Planetary growth with collisional fragmentation and gas drag. *Icarus* **209,** 836–847 (2010).
27. Senshu, H., Kuramoto, K. & Matsui, T. Thermal evolution of a growing Mars. *J. Geophys. Res.* **107,** 5118, doi:10.1029/2001JE001819 (2002).
28. Ricard, Y., Srámek, O. & Dubuffet, F. A multi-phase model of runaway core-mantle segregation in planetary embryos. *Earth Planet. Sci. Lett.* **284,** 144–150 (2009).
29. Caro, G., Bourdon, B., Halliday, A. N. & Quitté, G. Super-chondritic Sm/Nd ratios in Mars, the Earth and the Moon. *Nature* **452,** 336–339 (2008).
30. Debaille, V., Brandon, A. D., Yin, Q. Z. & Jacobsen, B. Coupled ^{142}Nd-^{143}Nd evidence for a protracted magma ocean in Mars. *Nature* **450,** 525–528 (2007).
31. Marty, B. & Marti, K. Signatures of early differentiation of Mars. *Earth Planet. Sci. Lett.* **196,** 251–263 (2002).
32. Pepin, R. O. On the origin and early evolution of terrestrial planet atmospheres and meteoritic volatiles. *Icarus* **92,** 2–79 (1991).
33. Dauphas, N. The dual origin of the terrestrial atmosphere. *Icarus* **165,** 326–339 (2003).

Supplementary Information is linked to the online version of the paper at www.nature.com/nature.

Acknowledgements Discussions with M. Chaussidon, H. Kobayashi, F. J. Ciesla, D. J. Stevenson, T. W. Dahl, R. Yokochi and G. Coutrot were appreciated. Comments from A. D. Brandon helped to improve the quality of the manuscript. We thank H. Kobayashi for sharing the digital outputs of his model simulations with us. The meteorite samples were provided by the Field Museum, the Smithsonian, the Muséum National d'Histoire Naturelle and R. N. Clayton. F. Marcantonio and P. J. Patchett gave us solutions of standards and spikes that were used to calibrate the measurements. This work was supported by a Packard fellowship, NASA and the NSF through grants NNX09AG59G and EAR-0820807 to N.D.

Author Contributions Both authors contributed equally to this work. N.D. and A.P. devised the method for purification and analysis of U, Th, Lu and Hf; A.P. performed the meteorite measurements; N.D. did the modelling; N.D. and A.P. wrote the paper.

Author Information Reprints and permissions information is available at www.nature.com/reprints. The authors declare no competing financial interests. Readers are welcome to comment on the online version of this article at www.nature.com/nature. Correspondence and requests for materials should be addressed to N.D. (dauphas@uchicago.edu).

METHODS

Details of sample digestion, elemental separations by TODGA extraction chromatography and multi-collector inductively coupled plasma mass spectrometer (MC-ICPMS) analysis have been published elsewhere[34]. Relatively unaltered meteorite chips of 100–500 mg (mainly observed falls) were sawn from larger pieces and cleaned for 10–20 s in an ultrasonic bath with a solution of 1 mol l^{-1} HCl (except for CI and E chondrites) followed by 10 s of sonication in high-purity ethanol. Dried sample pieces were crushed in an agate mortar and ~100 mg of the homogenized powder was directly weighed with ultra-pure lithium metaborate flux in a 8-ml high-purity graphite crucible (Spex CertiPrep) for alkali flux fusion. Flux:sample ratios ≥6 were required in order to achieve complete sample digestion and subsequent dissolution of the fusion melt. High-temperature flux fusion was preferred over acid dissolution to ensure that all refractory phases were completely digested. In order to achieve low-blank dissolution by flux melting, commercially available Puratronic lithium metaborate (99.997% metals basis, Alfa Aesar) was further purified according to the protocol presented in ref. 34. Approximately 100 ml of high-purity lithium bromide (LiBr) solution was also added as non-wetting agent to prevent adhesion of the flux to the graphite crucible and allow quantitative transfer of the melt.

The crucible was capped to minimize contamination and fusion was performed in a Thermolyne furnace at 1,070 °C for 12 min. The melt was transferred to a 30-ml Teflon PFA Savillex vial containing 25 ml of 3 mol l^{-1} HNO_3 and complete dissolution was typically achieved in a few minutes. The flux solution was spiked with a calibrated ^{236}U–^{229}Th–^{176}Lu–^{180}Hf spike solution for IDMS. After 4 h of sample–spike equilibration at 120 °C, the solution was directly loaded onto a pre-conditioned, 2-ml Eichrom TODGA cartridge for separation of the analytes from matrix elements by extraction chromatography. The TODGA resin has a very high affinity for actinides (U and Th), high-field strength elements (Hf) and rare earth elements (Lu) in 3 mol l^{-1} HNO_3 (refs 34, 35). Matrix elements were rinsed from the TODGA cartridge in 12 ml of 3 mol l^{-1} HNO_3, followed by 15 ml of 11 mol l^{-1} HNO_3. Subsequently, U, Th and Hf were eluted in 20 ml of 3 mol l^{-1} HNO_3 + 0.3 mol l^{-1} HF at 65 °C. Ytterbium and Lu were directly eluted onto a 2-ml Eichrom Ln cartridge in 0.5 mol l^{-1} HCl. The additional Ln chromatography step was needed to separate residual heavy rare earth elements (HREE) from Lu and Yb. Following the removal of HREE in 3.5 mol l^{-1} HCl, ~70% of Lu and ~30% of Yb were eluted in 20 ml of 6 mol l^{-1} HCl. The eluents, containing U–Th–Hf and Lu–Yb, were evaporated to near dryness and treated with a few drops of concentrated perchloric acid to eliminate potential organic molecules from the extraction resins. The residues were finally redissolved in 0.4 mol l^{-1} HNO_3 + 0.04 mol l^{-1} HF for U, Th and Hf, and 0.4 mol l^{-1} HNO_3 for Lu-Yb and were analysed on a Neptune MC-ICPMS at the Origins Laboratory of the University of Chicago.

About 90% of the U–Th–Hf solution was used for concentration and high-precision isotope analysis of Hf and the remaining 10% was used for the analysis of U and Th concentrations by IDMS. Samples were introduced to the Neptune instrument through an Apex-Q + Spiro TDM desolvation inlet system using a 100 µl min^{-1} PFA self-aspirating nebulizer. Uranium and Th concentration measurements were made in dynamic mode, with ^{236}U and ^{229}Th ion beams on the secondary electron multiplier (SEM) and ^{235}U, ^{238}U and ^{232}Th on Faraday collectors. Yield calibration between the SEM and Faraday cups was performed using the NIST4321c U standard solution (courtesy of F. Marcantonio, Texas A&M University), which has a $^{238}U/^{235}U$ ratio of 137.90. This ratio was also used for the calculation of mass bias by standard-sample-standard bracketing technique. Tail contributions (abundance sensitivity) from ^{238}U and ^{232}Th on lower-abundance isotopes were negligible. Procedural blanks were treated similarly to the samples and their contributions were determined by IDMS. Blank contributions for U and Th were measured at 10 pg and 13 pg, respectively. Hafnium and Lu blanks were 13 pg and 7 pg, respectively. The MC-ICPMS acquisition method for U, Th and Lu concentrations consisted of 1 block of 5 cycles of 4.2 s integration time. Each sample was analysed up to three times. Hafnium isotopic composition and concentration were established using a method that consisted of 1 block of 15 cycles of 8.4 s integration time to achieve higher precisions. The average $^{176}Hf/^{177}Hf$ ratio for JMC-475 ($n = 150$, courtesy of J. Patchett, University of Arizona) was 0.282159 ± 3 ($2\sigma/\sqrt{n}$). All $^{176}Hf/^{177}Hf$ ratios measured in meteorites from Table 1 were normalized to the conventionally accepted value of 0.282160 for JMC-475 (ref. 36). Although isobaric interferences on ^{180}Hf from ^{180}Ta and ^{180}W were minimal (<0.1%), these corrections were implemented. The details of concentration calculations and offline mass bias and interference corrections for Hf isotopes are presented in ref. 34. Because Lu has only two naturally occurring isotopes, Yb isotopes are commonly used to determine instrumental mass bias for Lu concentration measurements by isotope dilution[13,37–39]. Lutetium concentrations were calculated using the natural $^{173}Yb/^{171}Yb$ ratio of 1.132685 (ref. 37) for mass bias calculations. Uncertainties (95% confidence intervals) were calculated on the basis of seven replicate analyses of the Allende CV3 carbonaceous chondrite.

34. Pourmand, A. & Dauphas, N. Distribution coefficients of 60 elements on TODGA resin: application to Ca, Lu, Hf, U and Th isotope geochemistry. *Talanta* **81,** 741–753 (2010).
35. Horwitz, E. P., McAlister, D. R., Bond, A. H. & Barrans, R. E. Novel extraction of chromatographic resins based on tetraalkyldiglycolamides: characterization and potential applications. *Solvent Extract. Ion Exch.* **23,** 319–344 (2005).
36. Vervoort, J. D. & Blichert-Toft, J. Evolution of the depleted mantle: Hf isotope evidence from juvenile rocks through time. *Geochim. Cosmochim. Acta* **63,** 533–556 (1999).
37. Chu, N. C. *et al.* Hf isotope ratio analysis using multi-collector inductively coupled plasma mass spectrometry: an evaluation of isobaric interference corrections. *J. Anal. At. Spectrom.* **17,** 1567–1574 (2002).
38. Connelly, J. N., Ulfbeck, D. G., Thrane, K., Bizzarro, M. & Housh, T. A method for purifying Lu and Hf for analyses by MC-ICP-MS using TODGA resin. *Chem. Geol.* **233,** 126–136 (2006).
39. Vervoort, J. D., Patchett, P. J., Söderlund, U. & Baker, M. Isotopic composition of Yb and the determination of Lu concentrations and Lu/Hf ratios by isotope dilution using MC-ICPMS. *Geochem. Geophys. Geosyst.* **5,** Q11002, doi:10.1029/2004GC00072 (2004).